Why the Arc, and its Interactions with the Electrodes, Are Important in Predictive Modelling of Arc Welding

Murphy A. B.[1]

[1]CSIRO Manufacturing, PO Box 218, Lindfield NSW 2070, Australia, tony.murphy@csiro.au

The importance of two-way interactions between the arc and electrodes in welding is demonstrated by three examples: the influence of weld pool surface deformation on heat transfer, the momentum and energy transferred by droplets, and the effects of metal vapour on the arc and weld pool. It is concluded that a predictive model of arc welding requires the arc to be included in the computational domain. This will also facilitate calculation of properties such as microstructure and residual stress.

Keywords: arc welding, computational modelling, metal vapour, droplets, thermal plasma

1 INTRODUCTION

Arc welding is the most widely-used industrial thermal plasma process. An arc is struck in a shielding gas between two electrodes, one of which is the workpiece, i.e., the metal components that are joined by the welding process. The workpiece partially melts, forming a weld pool; when this solidifies, the components are bonded.

There are many types of arc welding. The most widely used in manufacturing is metal inert-gas (MIG) welding, in which the upper electrode is a metal wire, and the lower electrode is the workpiece. Usually the wire is the anode and the workpiece is the cathode. The tip of the wire melts to form droplets that pass through the arc into the weld pool.

Metal inert-gas welding is known as metal active-gas (MAG) welding when the shielding gas contains oxygen or carbon dioxide. Typical shielding gases are argon or helium in MIG welding, and argon-oxygen, argon–carbon dioxide or pure carbon dioxide in MAG welding. MIG/MAG welding is also known as gas metal arc welding (GMAW).

1.1 APPROACHES TO MODELLING OF ARC WELDING

The most important factor in arc welding is the properties of the welded joint. For this reason, the focus of arc welding models is the workpiece. Sophisticated models have been developed that predict properties including the weld depth and shape, the changes to microstructure resulting from the heating and cooling of the metal, and the residual stresses that develop in the workpiece.

Because of the focus on the workpiece properties, the great majority of computational models of arc welding do not include the arc or the wire electrode in the computational domain. The arc is taken into account only through boundary conditions at the surface of the workpiece and weld pool. This is a very significant simplification. However, determination of the boundary conditions representing the arc creates significant difficulties.

A typical example is provided by the approach of Zhang et al. [1], who assumed Gaussian distributions of the heat flux Q_a, electric current J_a and pressure P_a at the weld pool surface:

$$Q_a = \frac{\alpha IV}{2\pi R_q^2}\exp\left(-\frac{r^2}{2R_q^2}\right) - h_c\left(T_w - T_a\right),$$
$$P_a = \frac{F}{2\pi R_p^2}\exp\left(-\frac{r^2}{2R_p^2}\right), \qquad (1)$$
$$J_a = \frac{I}{2\pi R_q^2}\exp\left(-\frac{r^2}{2R_q^2}\right),$$

where I is the arc current, V is the arc voltage, r is the radial coordinate and T_w is the temperature of the workpiece surface. Six parameters have to be determined empirically or otherwise estimated: the efficiency of energy transfer α, a convective heat transfer coefficient h_c, the arc force F, the arc temperature adjacent to the workpiece T_a, and effective radii for heat transfer and pressure, R_q and R_p respectively. These parameters are typically estimated by comparing predictions of

the model against measurements, for example of weld depth and shape.

A less common approach to modelling of arc welding is to include the arc in the computational domain. This has the disadvantage that the model becomes much more complex, since the properties of the arc, and its interactions with the wire and workpiece, have to be calculated. However, if the arc is included self-consistently, then the boundary conditions between the arc and weld pool are determined by the model, and so do not have to be estimated.

1.2 OUTLINE OF PAPER

In this paper, I first describe the methods used in developing a computational model of MIG welding that includes the wire electrode and arc in the computational domain. I then present results that demonstrate the value of this approach. In particular, I show that the deformation of the weld pool surface, the transfer of energy and momentum by the droplets, and the production of metal vapour (a) are of great importance in determining the properties of the weld, and (b) can only be predicted accurately by including the arc and the wire electrode in the computational domain.

Finally, I consider the value of the second approach in predicting the microstructure of the heat-affected zone, and the residual stress in the workpiece, which are critical factors in determining the reliability of the weld.

2 THE COMPUTATIONAL MODEL

The computational model solves the equations of incompressible viscous flow, modified to include plasma effects and the conduction of electric current, in a computational domain that includes the wire electrode, the arc plasma, and the workpiece. The equations have been presented previously [1,2]; here a brief summary is provided.

The equations describe conservation of mass, momentum, energy and electric charge, with an additional equation to allow the magnetic potential to be determined from the current density. While the model can operate in either time-dependent or steady-state mode, only steady-state calculations are considered here.

The momentum and energy equations are transformed into the frame of reference of the wire electrode, which moves with respect to the fixed workpiece, using the approach of Mundra et al. [3].

The rate of vaporization of the electrode and weld pool is calculated self-consistently using the Hertz–Langmuir equation and depends on the local temperature of the wire electrode or weld pool surface and the mass fraction of the vapour in the adjacent plasma [2]. Modelling of the diffusion of the metal vapour required an additional conservation equation, for the mass fraction Y_M of metal species (atoms, ions and the electrons derived from metal atoms):

$$\nabla \cdot (\rho \boldsymbol{v} Y_M) = -\nabla \cdot \boldsymbol{J}_M = S_M, \qquad (2)$$

where ρ is the mass density, $\boldsymbol{v}$ is the flow velocity, S_M is the metal vapour source term (proportional to the rate of vaporization), and $\boldsymbol{J}_M$ is the diffusion mass flux, calculated using the combined diffusion coefficient approach, with is equivalent to the full multi-component approach [4].

The equations are solved in three-dimensional Cartesian geometry, using the finite volume method of Patankar [5], incorporating the SIMPLEC algorithm of van Doormaal and Raithby [6].

2.1 TREATMENT OF DROPLETS

Droplets are formed at the molten tip of the wire electrode. They detach and pass through the arc, transferring mass, momentum and energy to the weld pool. A full treatment of the droplet formation and transport requires a surface-tracking approach such as the volume-of-fluids method [7]; this is, however, highly computationally-intensive and is only applicable to time-dependent calculations..

A alternative time-averaged treatment of the influence of the droplets was developed [8]; this treatment is computationally much faster than the volume-of-fluids method, but still allows the influence of the droplets on the arc plasma and the weld pool to be determined. The temperature, velocity and diameter of the droplets are tracked from their detachment from the wire to their impact with the weld pool, with the heat, momentum and mass transfer determined using the PSI-CELL ap-

proach of Crowe et al. [9]. The effects of the droplets on the plasma and weld pool are taken into account using source terms averaged over the spatial extent of the droplets' path and over time. The main drawback of the approach is that changes in the shape of the tip of the wire as droplets form and detach are not considered.

2.2 INTERNAL BOUNDARIES

The internal boundaries between the electrodes and plasma, and between molten and solid metal, have to be treated carefully.

The latent heat of melting is taken into account at the liquid–solid interfaces using the method of Voller et al. [10]; this approach ensures numerical stability.

The shape of the free surface between the weld pool and the arc plasma is calculated by minimizing the total surface energy of the liquid metal, using the approach presented by Kim and Na [11]. This method takes into account the surface tension and surface curvature, the arc and droplet pressure, buoyancy in the weld pool, and the volume of metal transferred to the weld pool by droplets.

Four physical factors are important in determining the influence of the arc plasma on the weld pool: the heat flux, the current density, the arc pressure, and the shear stress applied by the plasma flow, all at the weld pool surface. Note that the first three of these parameters are typically defined as boundary conditions in models that do not include the arc in the computational domain, as per the example given in Eq. (1). In the model presented here, however, the parameters are determined self-consistently.

The workpiece is a non-thermionic cathode, for which the electron emission mechanism is not well understood. A simple expression is used for the heat flux [12] :

$$S = j\left(V_i - \varphi_w\right) - k\,\partial T/\partial x_{\perp}\,. \qquad (3)$$

The first term describes heating due to electron flux, and is the difference between sheath heating and the energy required to remove electrons from the metal; j is the current density, V_i is the sheath voltage, and φ_w is the work function of the metal. The second term is thermal conduction; k is the thermal conductivity, T is the temperature, and $x_{\perp}$ is position perpendicular to the workpiece surface.

The boundary conditions for momentum transfer across the arc–weld-pool interface parallel and perpendicular to the weld pool surface are respectively

$$\begin{aligned} &\tau_a - \tau_w + \left(d\gamma/dT\right)\left(dT/dx_{\mathrm{ll}}\right) = 0, \\ &P_a - P_w + \gamma\kappa = 0. \end{aligned} \qquad (4)$$

The parallel boundary condition states that the difference between the shear stresses in the arc τ_a and in the weld pool τ_w is determined by the Marangoni term $d\gamma/dx_{\mathrm{ll}}$, which describes the variation of the surface tension γ due to the gradients of temperature parallel to the weld pool surface. The perpendicular boundary condition states that the difference between the arc pressure P_a and weld pool pressure P_w is determined by the product of the surface tension and the surface curvature κ.

The heat flux to the wire anode is given by

$$S = j\varphi_w - k\,\partial T/\partial x_{\perp}\,, \qquad (5)$$

where the first term again describes heating due to electron flux (in this case electron condensation), and the second due to thermal conduction from the arc plasma.

2.3 THERMOPHYSICAL PROPERTIES

The thermophysical properties of the shielding gases, such as thermal conductivity and electrical conductivity, were taken from Murphy and Arundell [13] for argon, with properties for mixtures of argon and aluminium vapour calculated as described by Murphy [14].

Net radiative emission coefficients for argon were taken from Cram [15] and for aluminium from Essoltani et al. [16], with data for mixtures calculated based on mole fractions as recommended by Gleizes et al. [17].

3 RESULTS AND DISCUSSION

The computational model was run for bead-on-plate weld geometry, in which the workpiece is a flat plate, and the wire electrode is oriented vertically. Results obtained neglecting and including the influence of metal vapour are presented. The parameters used for the calculations are given in Table 1.

Table 1: Parameters used for calculations

Parameter	Value
Average arc current	95 A
Welding speed	15 mm s^{-1} (in $-y$ direction)
Wire diameter	1.2 mm
Wire feed rate	72 mm s^{-1}
Droplet frequency	93 s^{-1} (one-drop per pulse)
Arc length	5 mm (for flat workpiece)
Workpiece thickness	3 mm
Wire and workpiece alloy	AA5754 (Al + 3.1wt% Mg)
Shielding gas	Argon

3.1 DEFORMATION OF THE WELD POOL SURFACE

Droplets transfer molten metal from the wire to the weld pool, leading to an increase in the weld pool surface height. The arc tends to attach to the highest region of the weld pool, since this is typically the configuration that minimizes the arc voltage.

Fig.1 shows a comparison of the current density distributions predicted under the assumption that the weld pool surface remains flat, and by a calculation that includes the deformation of the surface due to the transfer of metal by droplets. In the former case, the current density distribution is approximately Gaussian, as per Eq. (1). In the latter case, the current density distribution is strongly asymmetric.

The current density distribution is critical in determining the heat flux to the weld pool, since the most important contribution to the heat transfer is the electron flux, which is proportional to the current density (see Eq. (3)).

This is an example of the importance of two-way interactions between the arc and the electrodes. The arc melts the wire and the workpiece, leading to droplet formation and a deformed weld pool. This in turn affects the location of the arc attachment, and thereby the transfer of energy from the arc to the weld pool.

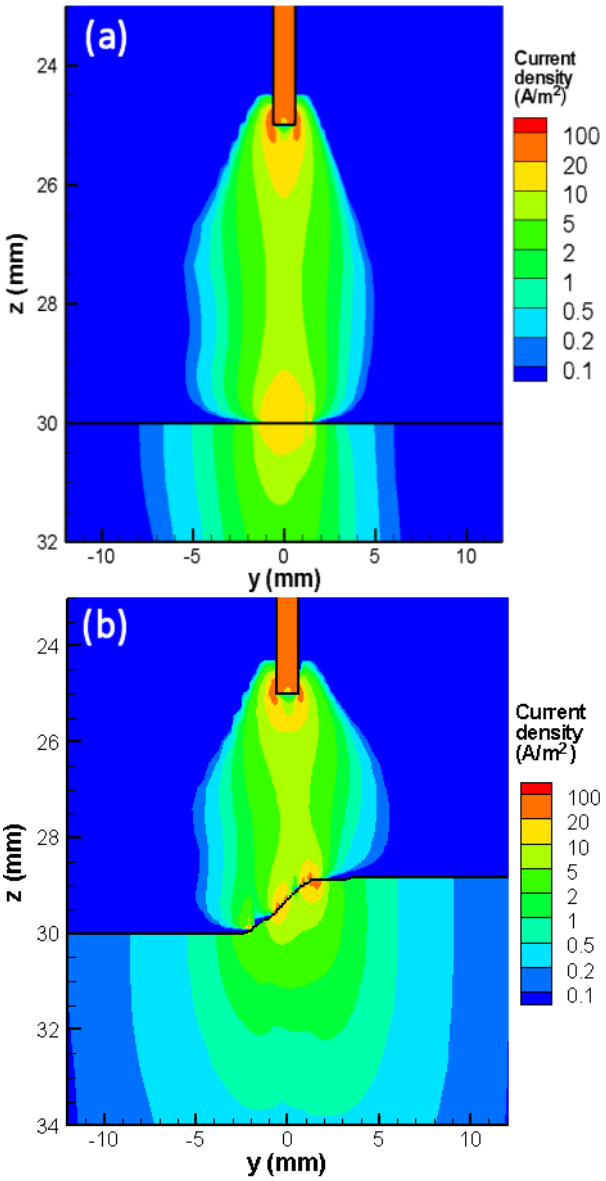

Fig.1: Current density distribution in a vertical cross-section through the wire, arc and workpiece: (a) assuming a flat weld pool surface, (b) including the deformation of the weld pool surface due to the transfer of metal by droplets; in both cases, metal vapour is neglected and the welding direction is to the left; from [1], © IOP Publishing; reproduced with permission; all rights reserved

3.2 DROPLETS

The momentum and heat energy transferred to the weld pool by the droplets have a large influence on the weld pool properties.

The initial temperature of the droplet is determined by the temperature of the tip of the wire when the droplet detaches. The initial velocity of the droplet is largely determined by the current density at the tip. Subsequently, heat and momentum are transferred to the droplet from the arc, since the temperature of the arc is

much higher than that of the droplet, and the plasma velocity is much higher than the droplet velocity [8].

Fig.2 shows the calculated radius, temperature and velocity of a droplet as it moves through the arc.

The influence of the droplet on the weld pool can be assessed by calculating the weld pool properties including and neglecting the transfer of momentum and energy by the droplet. The results are shown in Fig.3.

When all effects are taken into account, there is a strong downwards flow in the weld pool, starting at the position of droplet impact. However, when the droplet momentum is neglected, the flow is much weaker. When the droplet energy is neglected, the weld pool is significantly shallower.

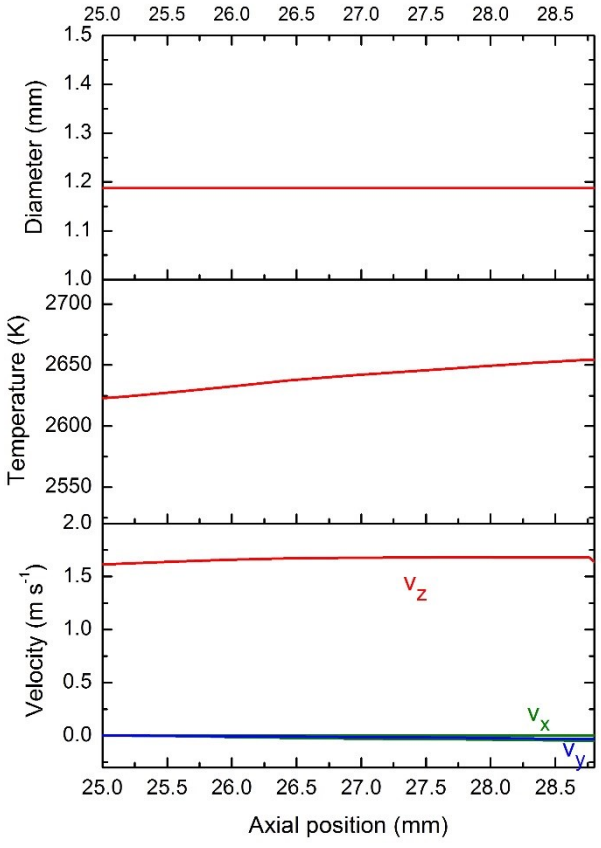

Fig.2: Diameter, temperature and components of the velocity of droplets as they pass through the arc from wire tip (at 25.0 mm) to the weld pool (at 28.75 mm); republished with permission of Maney Publishing from [8]; permission conveyed through Copyright Clearance Center, Inc.

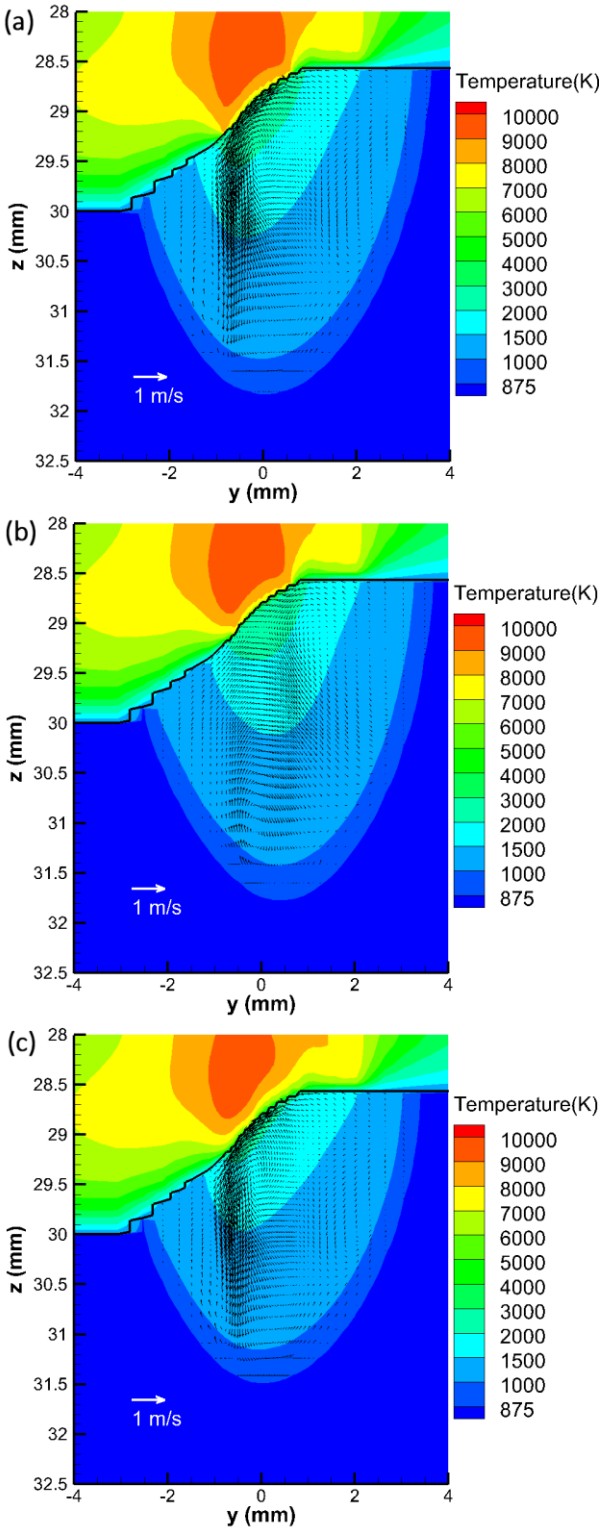

Fig.3: Vertical cross-section of weld pool, showing temperature distribution and velocity vectors, for (a) standard case, and cases in which (b) momentum, and (c) enthalpy, transferred by droplets is neglected; the welding direction is to the left; republished with permission of Maney Publishing from [8]; permission conveyed through Copyright Clearance Center, Inc.

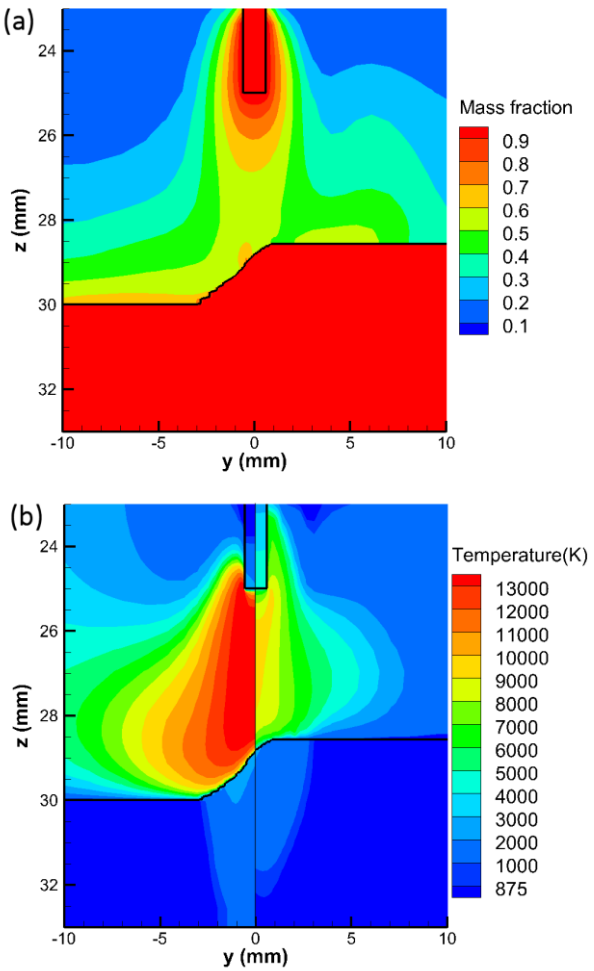

Fig.4: Distributions of (a) mass fraction of aluminium vapour, (b) temperature, in a vertical cross-section through the wire, arc and workpiece; in (b), the left-hand side shows temperature neglecting the influence of metal vapour, and the right-hand side shows temperature including the effects of metal vapour; the welding direction is to the left; from [2]; © IOP Publishing; reproduced with permission; all rights reserved

It is thus apparent that both the momentum and the energy transferred by the droplets make a significant contribution to the weld pool properties.

Droplets therefore provide a second example of the importance of two-way interactions between the arc and electrodes. The droplet momentum and energy are largely determined by the arc parameters, through the interaction of the arc with both the wire electrode and the droplets, and in turn the droplet momentum and energy influence the properties of the weld pool and therefore the weld.

3.3 METAL VAPOUR

Metal vapour, produced from the tip of the wire, the droplet and the weld pool, has a very significant influence on the arc temperature. Emission spectroscopy measurements performed in MIG welding arcs with steel electrodes have shown the existence of a local temperature minimum in the centre of the arc [18]. Modelling has demonstrated that this is mainly due to the strong radiative emission from iron vapour, which is concentrated around the arc axis [19].

In Fig.4, the predicted distribution of metal vapour in the arc, and the influence of the metal vapour on arc and weld pool temperature, are shown. The aluminium vapour is produced mainly from the wire tip, and is convected downwards by the strong flow in the arc; the flow velocity is over 100 m s^{-1} near the wire tip. The mass fraction of aluminum vapour is over 50% near the arc axis. The arc temperature is reduced due to the strong radiation from the aluminium vapour, and also because the temperature of the inflowing vapour is lower than that of the argon arc [2]. There is, however, no local temperature minimum, since aluminium vapour does not radiate as strongly as iron vapour, so the cooling is not as strong [2]. Recent laser-scattering measurements have confirmed the absence of a local temperature minimum in a MIG welding arc with aluminium electrodes [20].

Fig.5 shows a comparison of a measured weld cross-section with cross-sections predicted by the model both including and neglecting the influence of metal vapour. The presence of metal vapour significantly decreases the depth of the weld. This is partly due to the reduction in thermal conduction to the workpiece associated with the lower arc temperature, and partly to the decreased current density at the workpiece. The latter effect a consequence of the increased electrical conductivity of the plasma at low temperatures, which spreads out the arc attachment region. The increased conductivity at low temperatures is a consequence of the lower ionization enthalpy of aluminum atoms [14]. Eq. (3) shows both that both effects decrease the heat flux to the workpiece.

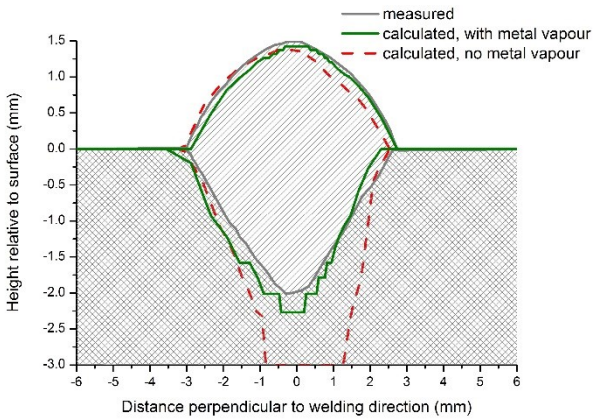

Fig.5: Comparison of measured weld cross-section (light-grey shaded region) with weld cross-sections calculated including (green solid line) and neglecting (red broken line) the effects of metal vapour; from [2]; © IOP Publishing; reproduced with permission; all rights reserved

Metal vapour provides a third example of the importance of two-way interactions between the arc and electrodes. The arc heats the wire and weld pool, leading to melting and vaporization of the metal; the metal vapour in turn affects the arc and the weld pool properties.

3.4 MICROSTRUCTURE AND RESIDUAL STRESS

While the weld depth and shape are of fundamental importance in welding, there are several other important factors, such as the residual stress in, and consequent deformation of, the welded metal, and the microstructure of the metal in the heat-affected zone. These factors are critical in determining the in-service reliability of the weld.

Modelling of residual stress and microstructure require thermal histories (the dependence of temperature on time) at every point in the workpiece. In standard approaches, which generally use finite-element models, the thermal history is calculated using a two-dimensional or three-dimensional heat source. An example of a two-dimensional heat source is given by the heat flux equation in Eq. (1). Three-dimensional heat sources are typically expressed as an ellipsoid, such as:

$$Q = \alpha VI \exp\left\{-\left[\left(\frac{x}{r_1}\right)^2 + \left(\frac{y}{r_2}\right)^2 + \left(\frac{z}{r_3}\right)^2\right]\right\} \quad (6)$$

where the r_i are the radii of the ellipsoid in the x, y and z directions. The free parameters α and r_i are usually determined by measuring thermal histories at several position in the workpiece with thermocouples, and fitting the measured values to those predicted by the model [21].

The MIG welding model presented in this paper allows accurate prediction of the thermal history at every point in the workpiece. An example is shown in Fig.6. Coupling the MIG welding model with residual stress and microstructure models would therefore allow prediction of these properties over a wide range of welding parameters, without the need for measurements of the thermal history in each case.

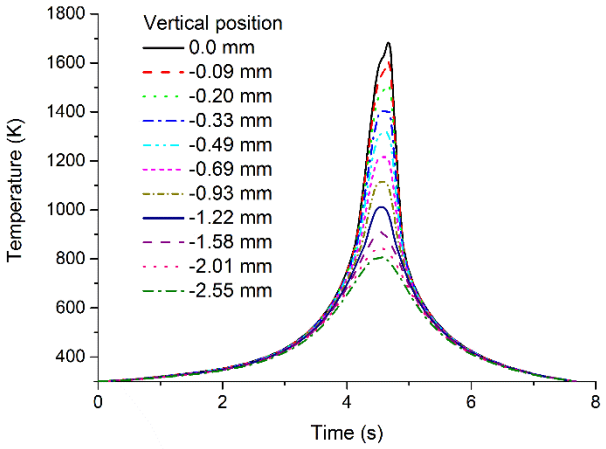

Fig.6 Thermal histories at different vertical positions in the workpiece on the arc axis; the vertical positions are measured from the top of the original workpiece surface, and correspond to those in Fig.5

4 CONCLUSIONS

I have presented three examples of two-way interactions between the arc and the electrodes in MIG welding: (1) the influence of deformation of the weld pool surface on transfer of energy from the arc to the weld pool; (2) the influence of the arc on droplet properties, which in turn affect the weld pool; and (3) the vaporization of the electrodes by the arc, and the consequent decrease in weld pool depth. In all three cases, it is only possible to predict the effects on the weld pool by including the arc in the computational domain. If the arc is instead represented by boundary conditions on the weld pool surface, the free parameters inherent in representation have to be re-

determined for every significant change in welding parameters.

A further advantage of including the arc in the computational domain is that reliable calculations of the thermal history of the workpiece can be performed. This data could be coupled to models that predict microstructure and residual stress in the workpiece, dispensing with the need for the use of heat sources that require calibration against measurements of temperature in the workpiece.

By including the arc and the wire electrode self-consistently within the computational domain, it should therefore be possible to develop a truly predictive model of arc welding, i.e., one in which repeated calibration against measurements is not required.

Acknowledgements

The support provided for the work reported here by General Motors, General Motors Holden, and the Commonwealth of Australia, through the AutoCRC, is gratefully acknowledged, as are useful discussions with Drs John Lowke, Eugene Tam, Vu Nguyen, Yuqing Feng and Dayalan Gunasegaram of CSIRO, and Dr Hui-Ping Wang of General Motors.

REFERENCES

[1] Murphy A B, J Phys D: Appl Phys 44 (2011) 194009.

[2] Murphy A B, J Phys D: Appl Phys 46 (2013) 224004.

[3] Mundra K, DebRoy T, Kelkar K M, Numer Heat Transfer A 29 (1996) 115-129.

[4] Murphy A B, Phys Rev E 48 (1993) 3594-3603.

[5] Patankar S V, Numerical Heat Transfer and Fluid Flow, Hemisphere, Washington DC 1980.

[6] van Doormaal J P, Raithby G D, Numer Heat Transfer 7 (1984) 147-163.

[7] Hirt C W, Nichols B D, J Comput Phys 39 (1981) 201-225.

[8] Murphy A B, Sci Technol Weld Join 18 (2013) 32-37.

[9] Crowe C T, Sharma M P, Stock D E, J Fluid Eng 99 (1977) 325-332.

[10] Voller V R, Prakash C, Int J Heat Mass Transfer 30 (1987) 1709-1719.

[11] Kim J-W, Na S-J, Weld J 74 (1995) 141s-152s.

[12] Lowke J J, Tanaka M, In: Proc. 17th International Conference on Gas Discharges and their Applications, Cardiff, UK, 7–12 September 2008. (Ed. Jones JE). 2008, 137-140.

[13] Murphy A B, Arundell C J, Plasma Chem Plasma Process 14 (1994) 451-490.

[14] Murphy A B, J Phys D: Appl Phys 43 (2010) 434001.

[15] Cram L E, J Phys D: Appl Phys 18 (1985) 401-411.

[16] Essoltani A, Proulx P, Boulos M I, Gleizes A, Plasma Chem Plasma Process 14 (1994) 437-450.

[17] Gleizes A, Cressault Y, Teulet P, Plasma Sources Sci Technol 19 (2010) 055013.

[18] Zielinska S, Musiol K, Dzierzega K, Pellerin S, Valensi F, de Izarra C, Briand F, Plasma Sources Sci Technol 16 (2007) 832-838.

[19] Schnick M, Fuessel U, Hertel M, Haessler M, Spille-Kohoff A, Murphy A B, J Phys D: Appl Phys 43 (2010) 434008.

[20] Kühn-Kauffeldt M, Marqués J-L, Schein J, J Phys D: Appl Phys 48 (2015) 012001.

[21] Muránsky O, Smith M C, Bendeich P J, Holden T M, Luzin V, Martins R V, Edwards L, Int J Sol Struct 49 (2012) 1045-1062.